



OPEN Identification of RBX1 as a regulator of LIPT1 transcription and its role in copper-induced cell death in GBM cells

Jianping Zeng^{1,6}, Jing Liu^{2,6}, Shushan Hua^{3,6}, Shuai Liu^{1,6}, Shoufang Tong⁴, Jie Zhang¹, Rajneesh Mungur⁵, Shangshi Chen¹, Jiugeng Feng¹ & Cong Ding¹✉

This study aimed to investigate the expression and prognostic significance of genes associated with copper-induced cell death in glioblastoma multiforme (GBM). Using a suite of bioinformatics tools and databases, the researchers analyzed gene expression, survival rates, and immune infiltration in GBM. Complementary *in vitro* experiments were performed to evaluate the effects of LIPT1 inhibition on GBM cell behavior in the context of copper-induced cell death. The team further explored upstream mechanisms leading to LIPT1 overexpression in GBM, specifically focusing on transcription factors and the role of ubiquitination degradation. The findings indicated a significant upregulation of LIPT1 in GBM, correlating with increased sensitivity to copper-induced cell death. Inhibition of LIPT1 was observed to exacerbate malignant behaviors in GBM cells post-copper exposure. Subsequent analysis pinpointed three transcription factors—CBX3, E2F6, and GTF2B—as regulators of LIPT1. Notably, GTF2B was also found to be co-expressed with LIPT1 and positively associated with recurrence-free survival in patients. ChIP-seq data analysis revealed significant GTF2B binding peaks near the LIPT1 promoter. Further exploration using UbiBrowser 2.0 identified E3 ubiquitin ligases that potentially target GTF2B, with RBX1 emerging as a viable anti-cancer target in GBM. Data from the UALCAN database showed a notable decrease in RBX1 protein expression in GBM tissues. Moreover, several ubiquitination modification sites were detected on the GTF2B protein. In conclusion, the study proposes a novel scientific hypothesis: RBX1 inhibits LIPT1 transcription by promoting the ubiquitin-mediated degradation of GTF2B, thereby suppressing copper-induced cell death in GBM cells. These findings offer new insights into the molecular mechanisms governing copper death sensitivity in GBM and identify potential therapeutic targets for further exploration.

Keywords Glioma, Cuproptosis, LIPT1, RBX1, GTF2B

Abbreviations

ChIP-seq	Chromatin immunoprecipitation sequencing
Co-IP	Co-immunoprecipitation
ChIP	Chromatin immunoprecipitation
CNS	Central nervous system
CRGs	Cuproptosis-associated genes
DFS	Disease-free survival
hTFtarget	The human transcription factors target
GBM	Glioblastoma multiforme

¹Department of Neurosurgery, The 1st Affiliated Hospital, Jiangxi Medical College, Nanchang University, Yong wai zheng Street 17, Nanchang 330006, Jiangxi Province, People's Republic of China. ²Department of Pharmacy, The 1st Affiliated Hospital, Jiangxi Medical College, Nanchang University, Nanchang 330006, Jiangxi Province, People's Republic of China. ³Center for Laboratory Medicine, Allergy center, Department of Transfusion medicine, Zhejiang Provincial People's Hospital, Hangzhou Medical College, Hangzhou 310014, Zhejiang, China. ⁴Department of Transfusion Medicine, Tiantai People's Hospital of Zhejiang Province (Tiantai Branch of Zhejiang Provincial People's Hospital, Hangzhou Medical College, Taizhou, Zhejiang, China. ⁵Department of Neurosurgery, The First Affiliated Hospital of Zhejiang University, Hangzhou 310000, Zhejiang Province, People's Republic of China. ⁶These authors contributed equally: Jianping Zeng, Jing Liu, Shushan Hua and Shuai Liu. ✉email: 785583469@qq.com

GEPIA	Gene expression profiling and interactive analyses
LIPT1	lipoyltransferase 1
OS	Overall survival
PD-1	Programmed death receptor-1
PD-L1	PD-1 ligand
RFS	Recurrence-free survival
TCA	Tricarboxylic acid
WB	Western blotting

According to the World Health Organization, glioblastoma multiforme (GBM) is one of the most lethal and aggressive brain tumors, affecting millions worldwide¹. The current treatment for GBM involves multimodal comprehensive therapy, including surgery, radiotherapy, chemotherapy, and targeted therapy, typically spanning a treatment period of approximately 6 weeks². However, due to the highly invasive nature of GBM cells, they easily infiltrate surrounding brain tissue, rendering complete tumor resection difficult. This challenge results in a high recurrence rate, with the majority of patients experiencing recurrence within two years of diagnosis³, and a 5-year average survival rate of less than 6%⁴. Furthermore, the neurological dysfunction and decreased quality of life caused by the tumor have a devastating impact on patients and their families. Current treatment modalities face challenges such as poor treatment efficacy and clinical prognosis, underscoring the urgent need to explore advanced treatment strategies and develop new therapeutic directions to improve patient outcomes.

The molecular mechanisms underlying the development of GBM remain incompletely understood, emphasizing the critical importance of investigating novel mechanisms to inhibit GBM malignant progression and identify new treatment strategies. A new study revealed a novel cell death mechanism termed “copper-induced cell death (cuproptosis),” which is dependent on mitochondrial respiration, a mechanism not previously described⁵. Novel cell death mechanisms often introduce new targets for tumor therapy. Studies have demonstrated that copper-induced cell death is closely associated with the prognosis of various tumors and the regulation of the tumor microenvironment. It can even predict the prognosis of patients receiving immunotherapy based on copper-induced cell death activity⁶. Therefore, inducing copper-induced cell death holds promise as a prospective tumor treatment method; however, its role in GBM remains unclear and warrants further investigation.

This study explores the relationship between the copper-induced cell death-regulating gene lipoyltransferase 1 (LIPT1) and the prognosis of GBM patients. It further investigates the role and molecular mechanisms of the RBX1/GTF2B/LIPT signaling pathway in regulating copper-induced cell death in GBM, offering new molecular targets for GBM treatment.

Materials and methods

UALCAN survival analysis

UALCAN is an interactive web-based software that can be used to perform analyses of tumor subgroup gene expression and survival⁷. A survival analysis with a P-value less than 0.05 was considered statistically significant.

Expression levels and survival analysis of hub genes in GBM

The association between hub gene expression and patient survival in glioblastoma (GBM) was assessed using the Gene Expression Profiling and Interactive Analyses (GEPIA) platform⁸. Expression data from 162 GBM tissues and 207 non-tumor controls were interrogated. Analyses employed built-in covariates (age, gender, TNM stage), with the option to incorporate additional factors such as molecular subtype. Prognostic significance was determined by correlating gene expression with clinical outcomes, including Overall Survival (OS) and Disease-Free Survival (DFS), to pinpoint prognostic biomarkers among the hub genes.

TIMER database analysis

TIMER is a database⁹ for systematic analysis of immune information of various types of tumors. The TIMER database contains data from a total of 10,897 samples of 32 cancers from TCGA and can assess the abundance of tumor immune infiltration. The “Gene” module was used to analyze the correlation between the expression level of LIPT1 and the abundance of immune cell infiltration in GBM.

Evaluation of transcription factors

The Human Transcription Factors Target (hTFtarget) database, which comprises information on 659 transcription factors obtained from 7,190 experimental samples¹⁰, was used to predict potentially valuable transcription factors.

The ChIP-seq database

The ChIP-seq database provides Chromatin Immunoprecipitation Sequencing (ChIP-seq) data for studying the relationship between transcription factors and DNA binding sites¹¹. The Cistrome Data Browser is a resource of ChIP-seq, ATAC-seq and DNase-seq data from humans and mice. It provides maps of the genome-wide locations of transcription factors, cofactors, chromatin remodelers, histone post-translational modifications and regions of chromatin accessible to endonuclease activity.

The UbiBrowser 2.0 database

UbiBrowser 2.0 served as a comprehensive repository for identifying potential E3-substrate interactions across the entire human proteome¹². Next, we utilized the internet-based platform UbiBrowser to forecast the potential targets of GTF2B.

Cell culture

The human glioblastoma cell lines U251, U118, and A172, as well as the normal control HA1800 cells, were supplied by G. F. Vande Woude from the Van Andel Research Institute in Grand Rapids, MI. Human peripheral blood CD8⁺ T cells were bought from Shanghai Jinyuan Biotechnology Co., Ltd. (China), and were immediately used for the experiment after purchase. These cells were cultured in Dulbecco's modified Eagle medium or RPMI-1640 (Human peripheral blood CD8⁺ T cells) supplemented with 10% fetal bovine serum and maintained in a 5% carbon dioxide environment at 37 °C in a cell culture incubator.

Quantitative real-time PCR

Total RNA was extracted from cells by using TRIzol reagent (Invitrogen, #15596018CN) following the manufacturer's protocol. A cDNA synthesis kit (Takara, #RR037A) was used for the synthesis of cDNA according to the manufacturer's instructions. RT-PCR was performed using a TB Green[®] Premix Ex Taq[™] II (Tli RNaseH Plus) from Takara (#RR820Q). Table 1 lists the primer sequences used for the Quantitative Real-Time PCR. The relative expression level of each target gene was normalized to the endogenous reference gene glyceraldehyde-3-phosphate dehydrogenase (GAPDH) and calculated using the comparative 2^{-ΔΔCt} method. All reactions were run in triplicate. The primer sequences used in this study are listed in Table 1.

Western blot assay

Cells were lysed, and the protein in the supernatant extracts was quantified using a BCA protein assay kit (Beyotime Institute of Biotechnology). The total cell lysates, fifty micrograms per lane, were resolved on sodium dodecyl sulfate-polyacrylamide gel electrophoresis gels. These were then transferred onto polyvinylidene fluoride membranes (Millipore, Billerica, MA, USA). The membranes were incubated with primary antibodies LIPT1 (Invitrogen, #PA5-106991, 1:1000), PDX1 (Proteintech, #20989-1-AP, 1:1000), RBX1 (Proteintech, #14895-1-AP, 1:500), GTF2B (Proteintech, #16467-1-AP, 1:1000), GAPDH (Proteintech, #60004-1-1 g, 1:2000) overnight at 4 °C. The following day, they were treated with a horseradish peroxidase-linked secondary anti-rabbit or anti-mouse antibody (Bio-Rad). Immunoreactivity was detected using enhanced chemiluminescence (Amersham Biosciences, Piscataway, NJ, USA) with a Chemidoc imaging system and Quantity One software (Bio-Rad). Densitometric analysis was performed using the Quantity One software. GAPDH served as a loading control.

ES-Cu induced copper death

GBM cells were treated with varying concentrations of ES-Cu (elesclomol: CuCl₂ = 1:1), specifically 1, 2, 8, 16, 32, 40, 64, and 128 nM. The treatment was carried out for different durations: 0, 1, 2, 3, and 4 h. Following this, the medium was replaced with fresh medium and the cells were cultured for an additional 24 h to observe the cytotoxicity induced by the metal ions.

EdU staining

The Cell-Light EdU Apollo567 In Vitro Kit (Ribo, #V0726) was utilized to detect DNA synthesis activity in GBM cells. Cells treated with ES-Cu were incubated with 40 μM EdU medium for 3 h. Following this, the cells were fixed with 4% paraformaldehyde and permeabilized with 0.5% TritonX-100. The Apollo fluorescent dyeing solution was then added and incubated at room temperature for 30 min in the dark. Subsequently, the Hoechst33342 dyeing solution was added and incubated for an additional 15 min in the dark. The number of EdU positive cells was observed using a fluorescence microscope.

Primer	Sequence(5' to 3')
Human GAPDH-F (RT-qPCR)	GTCTCCTCTGACTTCAACAGCG
Human GAPDH -R (RT-qPCR)	ACCACCCTGTTGCTGTAGCCAA
Human LIPT1 -F (RT-qPCR)	CAGGAACAGCTTCTAAGATCGGC
Human LIPT1-R (RT-qPCR)	AGCAGTGGCATTGCTCCTGATC
Human RBX1 -F (RT-qPCR)	ACTGTGCCATCTGCAGGAACCA
Human RBX1-R (RT-qPCR)	ACCTGTCGTGTTTTGAGCCAGC
Human GTF2B -F (RT-qPCR)	GATCTGTCCTGAATGTGGCTTGG
Human GTF2B-R (RT-qPCR)	GAGGATTCTGAGAATCTCCAACCT
Human LIPT1 shRNA#1	GCACTTGGGACGACCTAATTT
Human LIPT1 shRNA#2	ACACAGGAGGGAGGGTAAATA
Human LIPT1 shRNA#3	GTCCCAGCAGCTGGCTTTAAA
Human GTF2B shRNA #1	ATCAATCTACCTCGAAATATA
Human GTF2B shRNA #2	GCTTCTGCTTGTCTCTATATT
Human GTF2B shRNA #3	TGTGGCAGCGGACAGTATTTA
Human LIPT1-F (ChIP-qPCR)	AATTGCTTAAGGAAAATGTAAGTGTG
Human LIPT1-R (ChIP-qPCR)	TGTTAAAGAGTACAGCATGTTTGAG

Table 1. Primer sequences, shRNAs, and SiRNAs used in this study.

LIVE/DEAD cell imaging assay

The LIVE/DEAD™ cell imaging kit (Invitrogen, #R37601) was employed to analyze cell death following treatment with ES-Cu (40 nM, 3 h). Cells treated with ES-Cu were stained with the Live Green /Dead Red staining solution. This was followed by an incubation period at room temperature for 15 min in the dark. Observations were made under a fluorescence microscope. Living cells were colored green, while dead cells were colored red. The cell mortality rate was subsequently calculated based on these observations.

MTT assay

Following the induction of ES-Cu, a 10 μM MTT solution (5 mg/mL; Sigma-Aldrich) was added to each well containing GBM cells (5000 cells per well). After culture at 37 °C for 4 h, supernatant was discarded and 200 μL DMSO was introduced. Absorbance at 570 nm was obtained by a microplate reader (Varioskan LUX, Invitrogen, Waltham, MA, USA).

Colony formation assay

GBM cells were digested with trypsin and then inoculated into 6-well plates, with each well containing 2000 cells. After these cells were treated with 40 nM concentration of ES-Cu for 3 h, they were then cultured under normal conditions for another 7 days. Following this, the cells were fixed with 4% paraformaldehyde for 20 min and stained with a 0.2% crystal violet solution. Colonies consisting of more than 50 cells were counted using an inverted microscope (Leica Microsystems, Germany).

Transwell invasion assay

Transwell invasion assays were conducted using 24-well Matrigel-coated chambers (8-μm pore size) sourced from BD Biosciences. As per the manufacturer's protocol, cells were allowed to grow until they reached 75–80% confluence. Following this, they were serum-starved for a period of 24 h. Nonmotile cells were subsequently removed with a cotton swab. The cells remaining on the lower surface of the filter were fixed with cold methanol and stained with a 0.1% (w/v) crystal violet solution (Sigma).

Migration assay

Cell migration assays were performed using modified Boyden chambers (Transwell®, Corning Incorporated, NY, USA), in 24-well plates containing uncoated Transwell polycarbonate membrane filters (8-μm pores) separating the lower and upper chambers. 500 μL aliquots of the corresponding media (with FBS) were placed in the lower chamber. Transfected U251 and A172 cells were loaded and incubated in the upper chamber. The cells that migrated to the lower surface of the membrane filter were fixed and stained with 1% crystal violet solution for 30 min after gently removing the non-migratory cells from the upper surface of the membrane filter. The number of cells migrating to the lower surface was determined microscopically by counting five random visual fields per well.

CD8 + T cytotoxicity assay and enzyme linked immunosorbent assay (ELISA)

After GBM cells were treated with 40 nM ES-Cu for 3 h according to the instructions, 2×10^4 GBM cells and 2×10^5 CD8 + T cells (Jin Yuan Biotechnology Co., Ltd., China) were co-cultured in 6-well plates. Following a 24-hour incubation period, the toxicity of the CD8 + T cells was evaluated. This was done using a human IFN-γ ELISA assay kit (Abcam, Cambridge, UK) and an LDH cytotoxicity assay kit (Thermo Fisher, Waltham, MA, USA), with the procedures carried out according to the instructions provided with the kits. Interferon γ (IFN γ) level was tested with ELISA kits (Abcam, Cambridge, UK). In short, supernatant of each co-culture group was harvested. Next, each sample well was added with 100 μL enzyme conjugate and allowed for reaction at 37 °C for 30 min. Then, each well was introduced with 100 μL horseradish peroxidase substrate solution for color development at 37 °C for 20 min. Lastly, each well was added with 50 μL termination solution and the absorbance at 450 nm was assessed within 20 min¹³. CD8 + T cell cytotoxicity was assayed with lactate dehydrogenase (LDH) cytotoxicity kit (Thermo Fisher, Waltham, MA, USA). Cytotoxicity was measured following: $\text{Cytotoxicity}\% = \frac{(\text{Chemical-treated LDH activity} - \text{Spontaneous LDH activity})}{(\text{Maximum LDH activity} - \text{Spontaneous LDH activity})} \times 100\%$ ¹³.

Lentiviral cell infection

For lentiviral cell infection, specific shRNA lentiviral particles containing gene interference sequences or specific overexpressed lentiviral particles containing gene CDS sequences were procured from Gilman Biotechnology (Shanghai) Co., LTD (Table 1). Lentiviral expression vectors containing the corresponding sequences were constructed and co-transfected into 293 T cells using Lipofectamine 2000 and packaging plasmids (psPAX2, #12260, Addgene; pMD2.G, #12259, Addgene). The titer and infection efficiency were determined by observing the expression of GFP under a fluorescence microscope. Following several days of infection at appropriate multiplicities and screening with 2 μg/ml puromycin, the lentivirus-infected GBM cells were collected. The screening process continued until stable infected cells were obtained.

In vitro ubiquitination experiment

A label fusion expression plasmid of HA-RBX1, Myc-GTF2B, and Flag-ubiquitin was constructed. This was then transfected into 293T cells as per the requirements. A six-hour treatment with 10 μM MG132 was employed to inhibit the ubiquitination degradation of the protein. Co-immunoprecipitation (Co-IP) was carried out using the Pierce co-precipitation kit, following the instructions provided with the kit. Cell lysates were prepared and immobilized with AminoLink Plus conjugate resin. These were then immunoprecipitated overnight at 4 °C. Following this, the sample was eluted. The eluent was subsequently analyzed using Western Blotting.

Chromatin immunoprecipitation (ChIP)-qPCR

ChIP was performed using ChIP kit (Abcam, UK) with a specific immunoprecipitation antibody (Thermo Fisher, USA) or normal rabbit IgG antibody (Thermo Fisher, USA). PCR amplification of the precipitated DNA was performed. Table 1 lists the primer sequences used for the ChIP assay.

Statistical analysis

To analyze the data obtained from the experiments, each experiment was conducted at least three times, and the data was expressed as mean \pm standard error of the mean (SEM). The statistical analysis was performed using SPSS version 19.0 software for Windows (SPSS Inc, Chicago, USA). The comparison between two groups was performed using the two-tailed Student's *t*-test. Multiple-group comparison was analyzed using one-way or two-way ANOVA. The significant difference was considered when $P < 0.05$.

Results

Expression of copper death-related genes in GBM and prognostic significance

According to the literature, 13 Cuproptosis-associated genes (CRGs) have been identified. These include 7 pro-copper death genes (FDX1, LIAS, LIPT1, DLD, DLAT, PDHA1, and PDHB), 3 anti-copper death genes (MTF1, GLS, and CDKN2A), and 3 copper transporters (ATP7A, ATP7B, SLC31A1)⁵. We analyzed the expression levels of these CRGs in GBM using the UALCAN database, with a statistical significance threshold set at $p < 0.05$. We found that the expression levels of FDX1, LIPT1, CDKN2A and SLC31A1 genes in GBM were significantly elevated (Fig. 1A and D), while the expression levels of PDHA1 and GLS genes were significantly decreased (Fig. 1E and F). Following this, we performed a prognostic analysis (Group Cutoff by Quartile) on these 6 significantly differentially expressed CRGs using the GEPIA database. Our analysis indicates that only LIPT1 has a relatively good prognostic value. The analysis results show that patients with glioblastoma who have a high expression level of LIPT1 have a significantly longer recurrence-free survival period (RFS) (Fig. 1G). However, there is no statistically significant difference in overall survival rate (OS) between patients with high and low expression levels of LIPT1 (Fig. 1H). Furthermore, using the TIMER database, we predicted that LIPT1 expression was significantly positively correlated with CD8 + T cell infiltration in GBM (Fig. 1I).

The elevated expression of LIPT1 in GBM represents enhanced copper death sensitivity

RT-qPCR revealed that LIPT1 expression was significantly higher in GBM cell lines (U251, U118, A172) compared to the human normal astrocyte cell line HA1800 (Fig. 2A). For subsequent experiments, we selected the U251 and A172 cell lines, which exhibited higher LIPT1 expression. The classic inducers of copper death are the copper carrier drug elesclomol and CuCl₂ in a 1:1 combination. The combined use of elesclomol and CuCl₂ (ES-Cu) induced cell toxicity in a concentration- and time-dependent manner (Fig. 2B and C). Ultimately, we found that treatment with ES-Cu at a concentration of 40 nM for 3 h was optimal for inducing copper death. ES-Cu-induced cell toxicity could not be prevented by Z-VAD-FMK (an apoptosis inhibitor), necrostatin-1 (a necrosis inhibitor), or ferrostatin-1 (a ferroptosis inhibitor), but it could be rescued by tetrathiomolybdate (a copper death inhibitor) (Fig. 2D). This suggests that the cell death induced by ES-Cu is due to copper death. We infected GBM cells with lentiviral shRNA targeting LIPT1, which resulted in the inhibition of LIPT1 and FDX1 (Ferrodoxin-1, a critical mediator of cuproptosis) expression in GBM cells as detected by RT-qPCR or Western blotting (Fig. 2E-F). Following this, we observed a significant reduction in copper death sensitivity in LIPT1-inhibited GBM cells upon copper death induction (Fig. 2G). The high expression of LIPT1 in GBM is associated with enhanced copper death sensitivity, suggesting that targeting copper death in GBM may be a promising therapeutic strategy.

Inhibition of LIPT1 promotes malignant biological behavior of GBM cells after copper-induced cell death

Our clonogenic assay revealed that inhibiting LIPT1 led to an increase in cell survival following ES-Cu treatment (Fig. 3A). Moreover, inhibiting LIPT1 was found to enhance the migration and invasion activity of cells (Fig. 3B and C). We then co-cultured CD8 + T cells with GBM cells following ES-Cu treatment. By measuring the concentration of IFN- γ in the co-culture supernatant using ELISA, we found that knocking down LIPT1 in GBM cells resulted in a decrease in IFN- γ released by CD8 + T cells in the co-culture system (Fig. 3D). We used an LDH assay to directly evaluate CD8 + T cell-mediated cytotoxicity, and our results indicated that knocking down LIPT1 increased the resistance of GBM cells to CD8 + T cell-mediated cytotoxicity (Fig. 3E).

Upstream mechanism analysis of LIPT1

To delve deeper into the upstream mechanisms of LIPT1 overexpression in GBM, we procured the genes co-expressed with LIPT1 in GBM (exhibiting a significant positive correlation) from UALCAN (Fig. 4A). A list of transcription factors targeting LIPT1 was obtained from hTFtarget, and a cross-selection was performed with the co-expressed genes procured from UALCAN. This resulted in three intersecting factors: CBX3, E2F6, and GTF2B (Fig. 4B). By leveraging the ChIP-seq database Cistrome Data Browser, we selected the top five GTF2B ChIP-seq samples with the highest quality control. We observed significant binding peaks of GTF2B in proximity to the LIPT1 promoter across all sequenced data (Fig. 4C). Utilizing UbiBrowser 2.0, we predicted the E3 ubiquitin ligases targeting GTF2B (Fig. 4D). Among these, RBX1 emerged as a potential anticancer target in GBM¹⁴, and a notable decrease in RBX1 protein expression in GBM was predicted by UALCAN (Fig. 4E). Multiple ubiquitination modification sites were identified on the GTF2B protein according to the UbiBrowser 2.0 database (Fig. 4F).

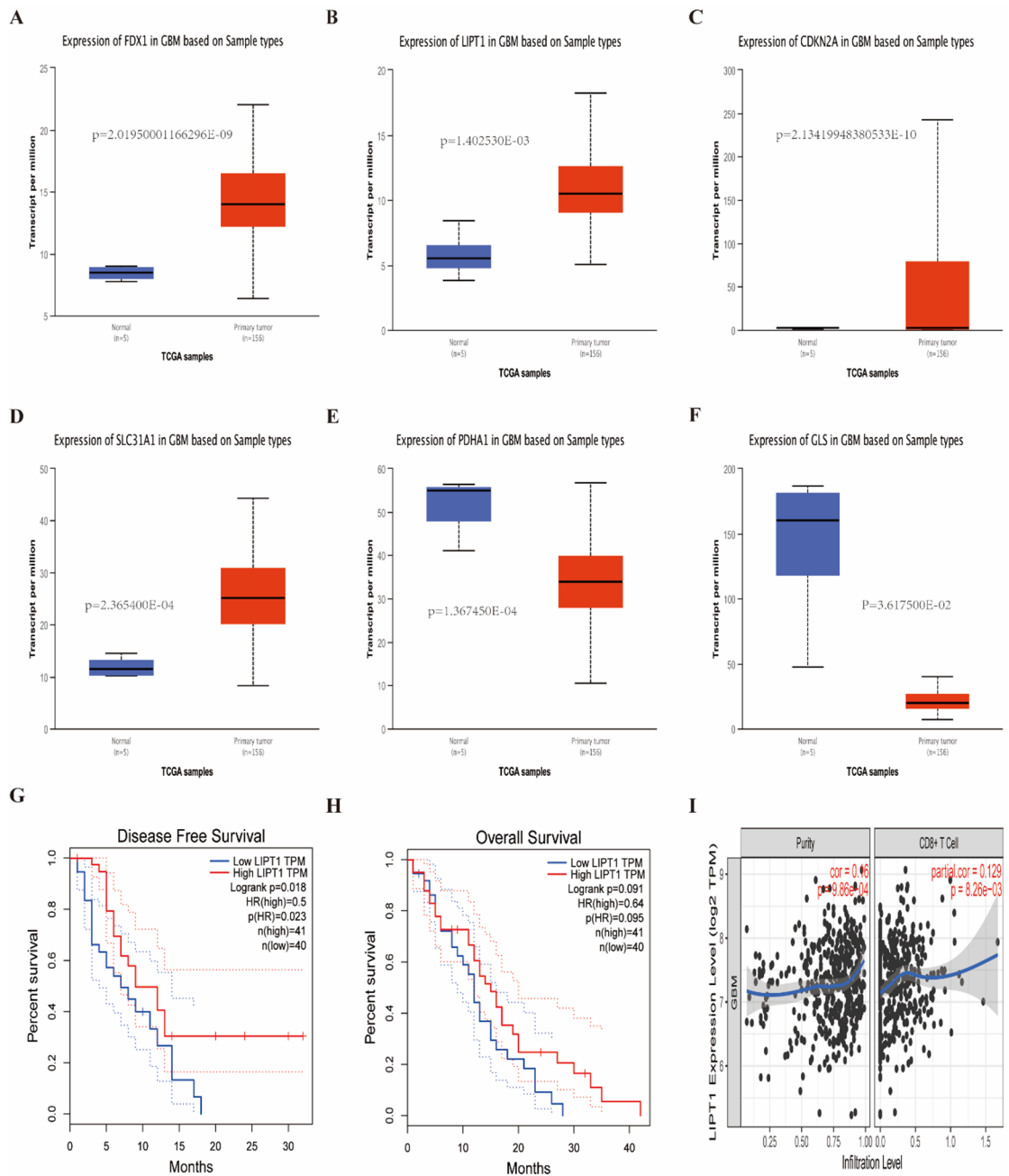


Fig. 1. Shows the comprehensive analysis of CRGs in GBM. (A–F) UALCAN identified significantly differentially expressed CRGs (FDX1, LIPT1, CDKN2A, SLC31A1, PDHA1, GLS) in GBM. (G–H) GEPIA analyzed the prognostic significance of LIPT1 expression on recurrence-free survival (RFS) and overall survival (OS) in GBM patients. I, TIMER database analyzed the correlation between LIPT1 expression and CD8 + T cell infiltration in GBM.

RBX1 ubiquitinates and degrades GTF2B to inhibit LIPT1 transcriptional expression

In the analysis of upstream mechanisms of LIPT1, through Western blot analysis, we found a significant decrease in RBX1 protein expression and a significant increase in GTF2B and LIPT1 expression in GBM cells compared to HA1800 cells (Fig. 5A). By lentiviral infection, we achieved stable overexpression of RBX1 or knockdown of GTF2B in GBM cell lines. Additionally, overexpression of RBX1 also led to a reduction in GTF2B protein expression (Fig. 5B). RT-qPCR analysis showed that both overexpression of RBX1 and knockdown of GTF2B resulted in a decrease in LIPT1 transcriptional expression in GBM cells. However, ubiquitinase inhibitor TAK-243 mitigated the LIPT1 transcriptional inhibition caused by the overexpression of RBX1 (Fig. 5C). The Western blot results further confirmed this finding (Fig. 5D). In vitro ubiquitination experiments demonstrated an interaction between RBX1 and GTF2B proteins, as overexpression of RBX1 increased the level of ubiquitination

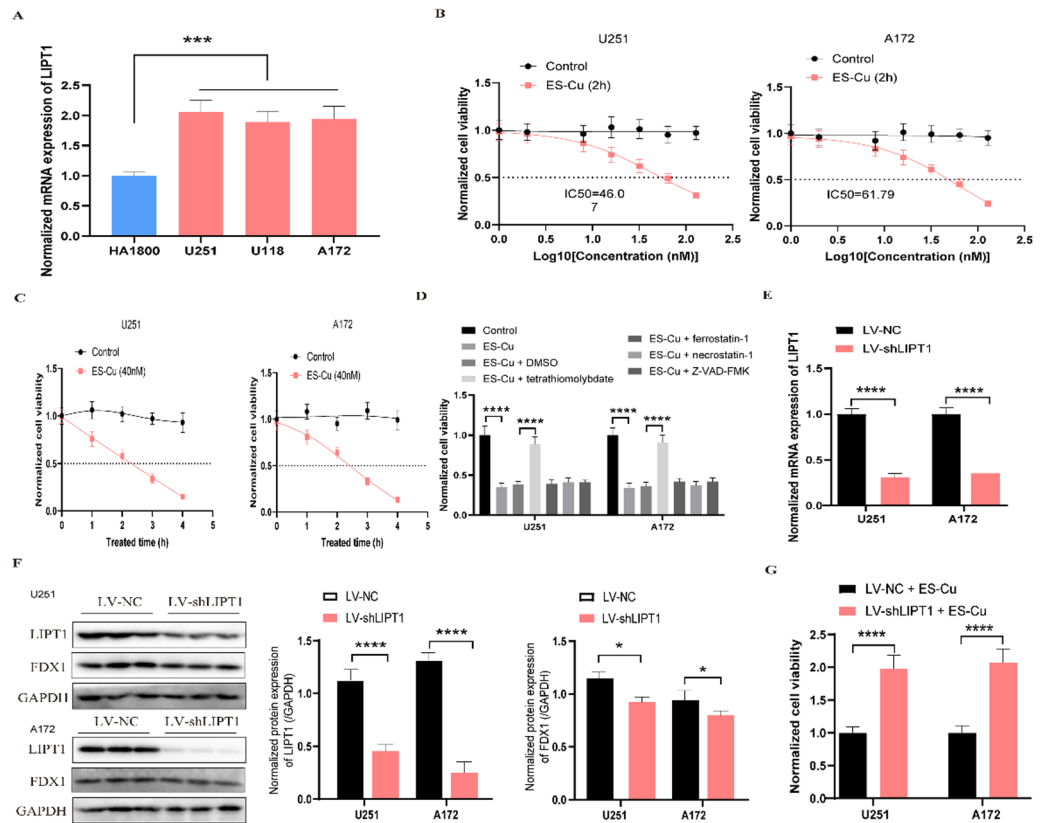


Fig. 2. LIPT1-mediated copper death sensitivity of GBM. (A) RT-qPCR detects the expression of LIPT1 in astrocyte HA1800 and GBM cell lines ($n = 3$, one-way ANOVA). (B) MTT detects the concentration-dependent toxicity of ES-Cu to GBM cells ($n = 3$, two-way ANOVA). (C) MTT detects the time-dependent toxicity of ES-Cu to GBM cells ($n = 3$, two-way ANOVA). (D) MTT detected the effect of different death inhibitors on ES-Cu-induced cytotoxicity ($n = 3$, one-way ANOVA). (E) RT-qPCR detects LIPT1 knockdown efficiency ($n = 3$, two-tailed student's *t*-test). (F) Western blot analysis shows the knockdown efficiency of LIPT1 and its effect on the expression of FDX1, a key cuproptosis marker protein ($n = 3$, two-tailed student's *t*-test). (G) MTT detected the effect of knockdown LIPT1 on ES-Cu-induced cytotoxicity ($n = 3$, two-tailed student's *t*-test). * $P < 0.05$, ** $P < 0.01$, *** $P < 0.001$, **** $P < 0.0001$.

modification on GTF2B protein (Fig. 5E). ChIP-qPCR experiments revealed that both overexpression of RBX1 and knockdown of GTF2B weakened the enrichment ability of GTF2B on the LIPT1 promoter (Fig. 5F).

Discussion

Traditionally, the central nervous system (CNS) has been commonly perceived as an immune-privileged site, characterized by few immune cells and limited immune activity¹⁵. However, recent studies have revealed that the human CNS exhibits robust immune activity¹⁶, opening avenues for immunotherapy in brain tumor treatment. Moreover, the heterogeneity of glioblastoma and its unique tumor immune microenvironment underscore the limitations of conventional therapies^{17,18}. This microenvironment comprises tumor-associated macrophages, myeloid-derived suppressor cells, and tumor-associated lymphocytes¹⁹, alongside blood-derived immune cells such as monocytes/macrophages, leukocytes, bone marrow stromal stem cells, dendritic cells, and lymphocytes, primarily CD4+, CD8 + T, regulatory T (Treg) cells, and NK cells²⁰. Locally produced cytokines, chemokines, and growth factors interact with extracellular matrix components, modulating the infiltrating immune cells. This interaction results in these cells acquiring different functional characteristics, thereby steering the immune system towards either a pro-inflammatory or anti-inflammatory response in GBM. Within this milieu, immune cells create a specialized ecosystem, pivotal in anti-tumor responses, immune regulation, and responses to therapeutic interventions²¹.

T cells are crucial for adaptive immunity. Copper regulates T cell function: Deficiency reduces IL-2 (vital for T cell differentiation, proliferation, and killing) production and mRNA in human T cells, reversible by supplementation^{22,23}. Combining copper chelation with anti-VEGF therapy inhibits mesothelioma by normalizing vasculature and increasing T-cell infiltration²⁴. Immunosuppressive Tregs (CD4+ subset) promote tumor immune escape^{25,26}. Inhibiting Treg infiltration in the tumor microenvironment (TME) improves immunotherapy response²⁷. Rapidly developing tumor immunotherapies (checkpoint blockade, vaccines, cell therapy) offer new hope. Copper's role in boosting anti-tumor immunity, particularly through the novel mechanism of cuproptosis, is driving research into copper-based strategies to improve immunotherapy²⁸.

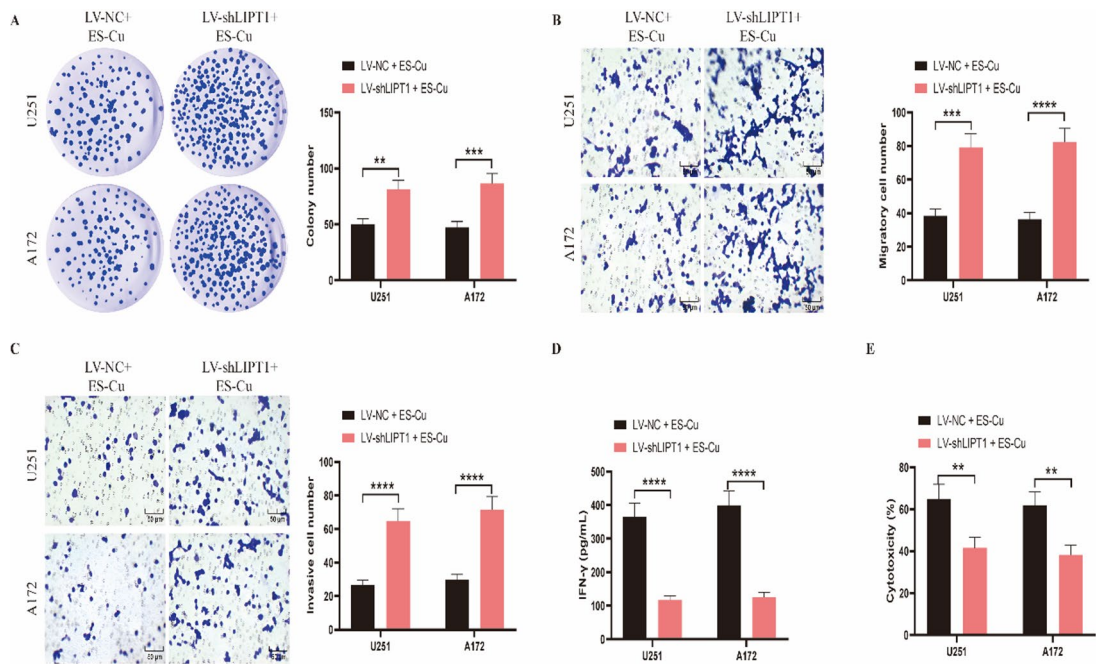


Fig. 3. Inhibition of LIPT1 Promotes the Malignant Biological Behavior of GBM Cells after Copper Death. (A) Clonalization assay detects the effect of LIPT1 knockdown on GBM cell survival after ES-Cu treatment ($n = 3$, two-tailed student's t-test). (B) Migration assay detects the effect of LIPT1 knockdown on GBM cell migration after ES-Cu treatment (40 nM, 3 h; $n = 3$, two-tailed student's t-test). (C) Transwell assay detects the effect of LIPT1 knockdown on GBM cell invasion after ES-Cu treatment ($n = 3$, two-tailed student's t-test). (D) ELISA assay detects the effect of LIPT1 knockdown on CD8 + T cell-mediated IFN- γ secretion in the co-culture system after ES-Cu treatment ($n = 3$, two-tailed student's t-test). (E) LDH assay detects the effect of LIPT1 knockdown on CD8 + T cell-mediated GBM cell cytotoxicity after ES-Cu treatment ($n = 3$, two-tailed student's t-test). * $P < 0.05$, ** $P < 0.01$, *** $P < 0.001$, **** $P < 0.0001$.

In recent years, the emergence of immune checkpoint inhibitors, particularly Programmed Death Receptor-1 (PD-1) monoclonal antibodies, has marked a significant shift in the field of cancer immunotherapy. However, the therapeutic efficacy of PD-1 monoclonal antibodies in treating glioblastoma has been found to be suboptimal, as indicated by the outcomes of completed Phase III clinical trials²⁹. Currently, Nivolumab, a PD-1 inhibitor, is under investigation in Phase III clinical trials. In these trials, 369 patients with recurrent GBM were randomly divided into two groups, receiving either 3 mg/kg of nivolumab or 10 mg/kg of bevacizumab, an anti-angiogenic drug targeting VEGF, every two weeks, with treatment continuing until confirmed disease progression. Preliminary findings from these trials suggest that the median survival and toxicity profiles of patients in the nivolumab group are comparable to those in the bevacizumab group³⁰. At present, given the presence of the blood-brain barrier, the complexity of GBM pathogenesis, the unique immune microenvironment in brain tissue, and the limitations of current biomolecular technologies, it becomes evident that further clinical studies may be required to fully harness the potential of GBM immunotherapy. Thus, while immunotherapy can serve as a component of a comprehensive treatment strategy, it cannot replace traditional surgical and radiation therapies. However, the potential for integrating traditional therapies with immunotherapy offers a promising avenue for the development of more effective treatment approaches.

Cuproptosis, an emerging mechanism of cell death, has become a focal point in the field of cancer research. The mechanism of cuproptosis is significantly different from known cell apoptosis, pyroptosis, necroptosis, and ferroptosis. It is a copper-dependent cell death process that is intricately linked to mitochondrial respiration: excess copper ions in cells can be transported to mitochondria by ion carriers, directly bind to the acylated components in the tricarboxylic acid (TCA) cycle of mitochondrial respiration, and also interfere with iron-sulfur clusters. Consequently, this interference results in the aggregation of acylated proteins and the loss of iron-sulfur cluster proteins, inducing protein toxicity stress and ultimately culminating in cell death^{5,31}. Elevated concentrations of copper ions have been observed in the serum and tumor tissues of patients with various malignant tumors, compared to serum and tissues of healthy individuals³². Additionally, studies from several universities and research institutions have suggested a potential correlation between the expression of cuproptosis-related genes, the immune microenvironment of gliomas^{33,34}, and patient prognosis^{35,36}. Therefore, the conclusions drawn from existing literature primarily rely on bioinformatics analysis and lack specific experimental validation. Thus, further exploration of the anti-tumor mechanism of cuproptosis holds substantial promise for future applications.

Based on published literature^{37,38} and data from bioinformatics platforms UALCAN⁷ and GEPIA⁸, we performed an analysis to predict the expression and prognostic significance of 13 copper death-related genes

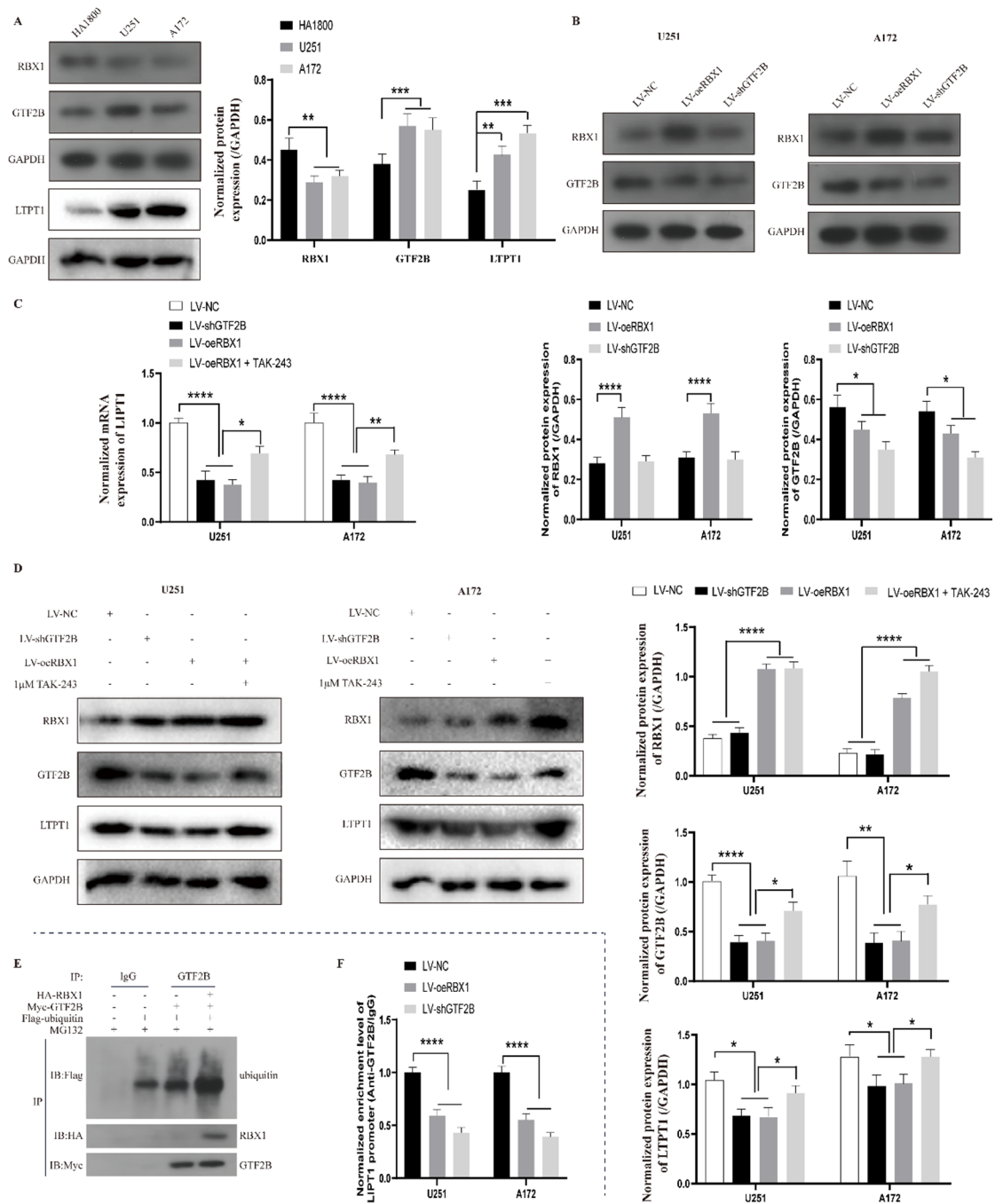


Fig. 5. The results of the signal conduction analysis of the RBX1/GTF2B/LIPT1 axis. **(A)** Protein expression of RBX1, GTF2B and LIPT1 in astrocyte HA1800 and GBM cell lines detected by WB ($n = 3$, two-way ANOVA). **(B)** Impact of RBX1 overexpression or GTF2B knockdown on RBX1 and GTF2B protein expression in GBM cells assessed by WB ($n = 3$, two-way ANOVA). **(C)** Effects of RBX1 overexpression or GTF2B knockdown on LIPT1 mRNA expression in GBM cells analyzed by RT-qPCR ($n = 3$, two-way ANOVA). **(D)** Effects of RBX1 overexpression or GTF2B knockdown on LIPT1 mRNA expression in GBM cells analyzed by WB ($n = 3$, two-way ANOVA). **(E)** In vitro ubiquitination assay to study RBX1-mediated ubiquitination of GTF2B protein ($n = 3$). **(F)** Enrichment of GTF2B on the LIPT1 promoter affected by RBX1 overexpression or GTF2B knockdown assessed by ChIP-qPCR ($n = 3$, two-way ANOVA). * $P < 0.05$, ** $P < 0.01$, *** $P < 0.001$, **** $P < 0.0001$.

(CRGs) in glioblastoma multiform. Our research revealed that, despite the elevated expression of the predicted LIPT1 in cancer tissues compared to normal tissues, only LIPT1 with high expression has notable prognostic value. Specifically, in GBM patients, high LIPT1 expression is associated with a significant improvement in recurrence-free survival (RFS) and a certain degree of increase in overall survival. The study found that in patients with low-grade gliomas, LIPT1 expression is also elevated in tumor tissues³⁹. In melanoma, LIPT1

expression significantly correlates with the infiltration of various immune cells and patient prognosis²⁷. A pan-cancer analysis also revealed that abnormal LIPT1 expression is associated with the infiltration of immune cells, including B cells, CD8 + T cells, and cancer-associated fibroblasts⁴⁰. This study also found that the expression of LIPT1 is positively correlated with the infiltration of CD8 + T cells. Therefore, we propose that the upregulation of LIPT1 expression in GBM may represent a self-defense mechanism of the body against GBM, specifically by enhancing the level of cellular cuproptosis, and mediating the infiltration of immune cells, thereby inhibiting GBM progression.

Utilizing the MTT assay, we discovered that by downregulating LIPT1 expression, we could significantly decrease the cuproptosis sensitivity of GBM cells, thereby enhancing cell viability. To further investigate this, we conducted clonogenic and Transwell invasion assays. These assays allowed us to examine the clonogenicity, migration, and invasion capabilities of GBM cells following LIPT1 downregulation. We found a significant enhancement in their malignant phenotype. Moreover, we discovered a negative correlation between the expression of LIPT1 and PD-L1 (PD-1 ligand) within GBM. Interestingly, co-culturing GBM cells with low LIPT1 expression and CD8 + T cells significantly reduced the release of IFN- γ and the cytotoxicity of GBM cells. Previous research has confirmed that mutations in LIPT1 can impair mitochondrial protein acylation and the TCA cycle⁴¹.

Research on pituitary adenomas has revealed that GTF2B can influence the tumor phenotype by modulating the expression of AIP protein⁴². In colorectal cancer research, it has been identified that the long non-coding RNA LINC00355 can promote the malignant phenotype of cancer cells by recruiting GTF2B to enhance ITGA2 expression⁴³. Utilizing the Cistrome Data Browser database we predicted and identified a binding peak of GTF2B in the vicinity of the LIPT1 promoter. However, it remains unclear whether GTF2B participates in the cuproptosis process of GBM cells by promoting LIPT1 transcription and the specific mechanism involved. To investigate the upstream mechanisms initiating a LIPT1-related spontaneous anti-tumor immune response in GBM, we downloaded genes co-expressed with LIPT1 in GBM from the UALCAN database and intersected them with transcription factors targeting LIPT1 from the hTFtarget¹⁰ database. Among these three intersecting factors, we identified the Transcription Factor IIB (GTF2B), whose role in GBM has not yet been reported. Further bioinformatics predictions indicated that, similar to LIPT1, the expression level of GTF2B in GBM is significantly higher than in normal tissues. However, patients with high GTF2B expression typically have a higher RFS.

Current research has clearly demonstrated that the regulation of protein degradation plays a pivotal role in the initiation and progression of tumors. It has been confirmed by prior studies that pertinent post-translational modifications could serve as potential therapeutic targets for GBM^{44,45}. Among these modifications, protein ubiquitination, a reversible process, is particularly noteworthy⁴⁶. Utilizing bioinformatics databases, we have predicted that RBX1, an upstream E3 ubiquitin ligase of GTF2B, is of utmost significance, and its expression in GBM is markedly reduced. Following a one-week treatment of GBM cells with temozolomide, we observed substantial DNA damage. Our bioinformatics analysis revealed a significant association between RBX1 and DNA damage repair, suggesting a potential connection between RBX1 and chemoresistance mechanisms in GBM⁴⁷. In this study, using in vitro cell models, we confirmed the pronounced downregulation of RBX1 in GBM cell lines, and RBX1 can control the ubiquitination of GTF2B. The latter regulates the cuproptosis sensitivity of GBM cells by activating the transcription of LIPT1.

Conclusions

Our finding suggest that RBX1 plays a pivotal role in mediating copper-induced cell death in GBM cells by regulating the ubiquitin degradation of GTF2B and enhancing LIPT1 transcription (Fig. 6). This study lays the groundwork for identifying potential therapeutic targets for GBM treatment and offers valuable insights and directions for the integration of targeted therapy with immunotherapy in the context of GBM.

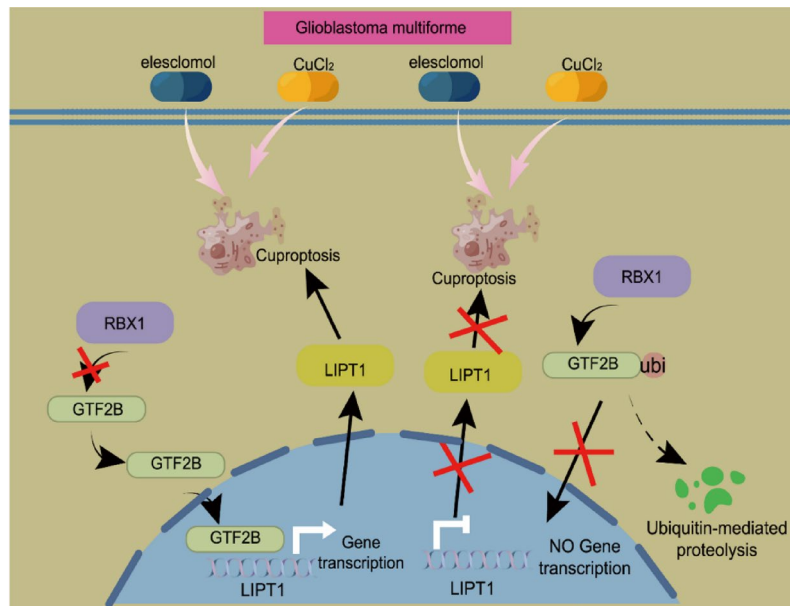


Fig. 6. The hypothesis mechanism diagram of the study. Reducing RBX1-mediated ubiquitination degradation of GTF2B in GBM can enhance the transcriptional activation of GTF2B on LIPT1, thereby promoting LIPT1 expression and increasing the copper death sensitivity of GBM.

Data availability

The datasets used and/or analyzed during the current study are available from the corresponding author on reasonable request.

Received: 5 January 2025; Accepted: 19 January 2026

Published online: 31 January 2026

References

- Muir, M., Gopakumar, S., Traylor, J., Lee, S. & Rao, G. Glioblastoma multiforme: novel therapeutic targets. *Expert Opin. Ther. Targets*. **24**, 605–614. <https://doi.org/10.1080/14728222.2020.1762568> (2020).
- Khabibov, M. et al. Signaling pathways and therapeutic approaches in glioblastoma multiforme (Review). *Int. J. Oncol.* **60** <https://doi.org/10.3892/ijo.2022.5359> (2022).
- Uddin, M. S. et al. Epigenetics of glioblastoma multiforme: from molecular mechanisms to therapeutic approaches. *Semin Cancer Biol.* **83**, 100–120. <https://doi.org/10.1016/j.semcancer.2020.12.015> (2022).
- Batash, R., Asna, N., Schaffer, P., Francis, N. & Schaffer, M. Glioblastoma Multiforme, diagnosis and Treatment; recent literature review. *Curr. Med. Chem.* **24**, 3002–3009. <https://doi.org/10.2174/0929867324666170516123206> (2017).
- Tsvetkov, P. et al. Copper induces cell death by targeting lipoylated TCA cycle proteins. *Science* **375**, 1254–1261. <https://doi.org/10.1126/science.abf0529> (2022).
- Xie, J., Yang, Y., Gao, Y. & He, J. Cuproptosis: mechanisms and links with cancers. *Mol. Cancer*. **22**, 46. <https://doi.org/10.1186/s12943-023-01732-y> (2023).
- Chandrashekar, D. S. et al. An update to the integrated cancer data analysis platform. *Neoplasia* **25**, UALCAN, 18–27. <https://doi.org/10.1016/j.neo.2022.01.001> (2022).
- Li, C., Tang, Z., Zhang, W., Ye, Z. & Liu, F. GEPIA2021: integrating multiple deconvolution-based analysis into GEPIA. *Nucleic Acids Res.* **49**, W242–w246. <https://doi.org/10.1093/nar/gkab418> (2021).
- Li, T. et al. TIMER2.0 for analysis of tumor-infiltrating immune cells. *Nucleic Acids Res.* **48**, W509–w514. <https://doi.org/10.1093/nar/gkaa407> (2020).
- Zhang, Q. et al. hTFtarget: A comprehensive database for regulations of human transcription factors and their targets. *Genomics Proteom. Bioinf.* **18**, 120–128. <https://doi.org/10.1016/j.gpb.2019.09.006> (2020).
- Yang, J. H., Li, J. H., Jiang, S., Zhou, H. & Qu, L. H. ChIPBase: a database for decoding the transcriptional regulation of long non-coding RNA and MicroRNA genes from ChIP-Seq data. *Nucl. Acids Res.* **41**, D177–187. <https://doi.org/10.1093/nar/gks1060> (2013).
- Wang, X. et al. UbiBrowser 2.0: a comprehensive resource for proteome-wide known and predicted ubiquitin ligase/deubiquitinase-substrate interactions in eukaryotic species. *Nucleic Acids Res.* **50**, D719–d728. <https://doi.org/10.1093/nar/gkab962> (2022).
- Tian, P., Wei, J. X., Li, J., Ren, J. K. & Yang, J. J. LncRNA SNHG1 regulates immune escape of renal cell carcinoma by targeting miR-129-3p to activate STAT3 and PD-L1. *Cell. Biol. Int.* **45**, 1546–1560. <https://doi.org/10.1002/cbin.11595> (2021).
- Jia, L., Soengas, M. S. & Sun, Y. ROC1/RBX1 E3 ubiquitin ligase Silencing suppresses tumor cell growth via sequential induction of G2-M arrest, apoptosis, and senescence. *Cancer Res.* **69**, 4974–4982. <https://doi.org/10.1158/0008-5472.Can-08-4671> (2009).
- Engelhardt, B., Vajkoczy, P. & Weller, R. O. The movers and shapers in immune privilege of the CNS. *Nat. Immunol.* **18**, 123–131. <https://doi.org/10.1038/ni.3666> (2017).
- Sampson, J. H., Maus, M. V. & June, C. H. Immunotherapy for brain tumors. *J. Clin. Oncol.* **35**, 2450–2456. <https://doi.org/10.1200/jco.2017.72.8089> (2017).
- Huang, B. et al. Current immunotherapies for glioblastoma multiforme. *Front. Immunol.* **11**, 603911. <https://doi.org/10.3389/fimmu.2020.603911> (2020).
- Medikonda, R., Dunn, G., Rahman, M., Fecci, P. & Lim, M. A review of glioblastoma immunotherapy. *J. Neurooncol.* **151**, 41–53. <https://doi.org/10.1007/s11060-020-03448-1> (2021).

19. Ou, A., Yung, W. K. A. & Majd, N. Molecular mechanisms of treatment resistance in glioblastoma. *Int. J. Mol. Sci.* **22** <https://doi.org/10.3390/ijms22010351> (2020).
20. Grabowski, M. M. et al. Immune suppression in gliomas. *J. Neurooncol.* **151**, 3–12. <https://doi.org/10.1007/s11060-020-03483-y> (2021).
21. Kaminska, B., Ochocka, N. & Segit, P. Single-Cell omics in dissecting immune microenvironment of malignant Gliomas- Challenges and perspectives. *Cells* **10** <https://doi.org/10.3390/cells10092264> (2021).
22. Lan, L., Feng, Z., Liu, X. & Zhang, B. The roles of essential trace elements in T cell biology. *J. Cell. Mol. Med.* **28**, e18390. <https://doi.org/10.1111/jcmm.18390> (2024).
23. Abbas, A. K., Trotta, E., Marson, D. R. S., Bluestone, J. A. & A. & Revisiting IL-2: biology and therapeutic prospects. *Sci. Immunol.* **3** <https://doi.org/10.1126/sciimmunol.aat1482> (2018).
24. Crowe, A., Jackaman, C., Beddoes, K. M., Ricciardo, B. & Nelson, D. J. Rapid copper acquisition by developing murine mesothelioma: decreasing bioavailable copper slows tumor growth, normalizes vessels and promotes T cell infiltration. *PLoS One.* **8**, e73684. <https://doi.org/10.1371/journal.pone.0073684> (2013).
25. Tanaka, A. & Sakaguchi, S. Regulatory T cells in cancer immunotherapy. *Cell. Res.* **27**, 109–118. <https://doi.org/10.1038/cr.2016.151> (2017).
26. Vinay, D. S. et al. Immune evasion in cancer: mechanistic basis and therapeutic strategies. *Semin. Cancer Biol.* **35** Suppl, S185–s198. <https://doi.org/10.1016/j.semcancer.2015.03.004> (2015).
27. Lv, H. et al. Comprehensive analysis of Cuproptosis-Related genes in immune infiltration and prognosis in melanoma. *Front. Pharmacol.* **13**, 930041. <https://doi.org/10.3389/fphar.2022.930041> (2022).
28. Zeng, J. et al. Cuproptosis in microsatellite stable colon cancer cells affects the cytotoxicity of CD8(+T) through the WNT signaling pathway. *Chem. Biol. Interact.* **403**, 111239. <https://doi.org/10.1016/j.cbi.2024.111239> (2024).
29. Mahmoud, A. B. et al. Advances in immunotherapy for glioblastoma multiforme. *Front. Immunol.* **13**, 944452. <https://doi.org/10.3389/fimmu.2022.944452> (2022).
30. Reardon, D. A. et al. Effect of nivolumab vs bevacizumab in patients with recurrent glioblastoma: the checkmate 143 phase 3 randomized clinical trial. *JAMA Oncol.* **6**, 1003–1010. <https://doi.org/10.1001/jamaoncol.2020.1024> (2020).
31. Chen, L., Min, J. & Wang, F. Copper homeostasis and Cuproptosis in health and disease. *Signal. Transduct. Target. Ther.* **7**, 378. <https://doi.org/10.1038/s41392-022-01229-y> (2022).
32. Michniewicz, F. et al. Copper: an intracellular achilles' heel allowing the targeting of Epigenetics, kinase Pathways, and cell metabolism in cancer therapeutics. *ChemMedChem* **16**, 2315–2329. <https://doi.org/10.1002/cmdc.202100172> (2021).
33. de Visser, K. E. & Joyce, J. A. The evolving tumor microenvironment: from cancer initiation to metastatic outgrowth. *Cancer Cell.* **41**, 374–403. <https://doi.org/10.1016/j.ccell.2023.02.016> (2023).
34. Kao, K. C., Vilbois, S., Tsai, C. H. & Ho, P. C. Metabolic communication in the tumour-immune microenvironment. *Nat. Cell Biol.* **24**, 1574–1583. <https://doi.org/10.1038/s41556-022-01002-x> (2022).
35. Chen, S. et al. Prognostic value of cuproptosis-related genes signature and its impact on the reshaped immune microenvironment of glioma. *Front. Pharmacol.* **13**, 1016520. <https://doi.org/10.3389/fphar.2022.1016520> (2022).
36. Wang, W. et al. The cuproptosis-related signature associated with the tumor environment and prognosis of patients with glioma. *Front. Immunol.* **13**, 998236. <https://doi.org/10.3389/fimmu.2022.998236> (2022).
37. Liu, H. Pan-cancer profiles of the Cuproptosis gene set. *Am. J. Cancer Res.* **12**, 4074–4081 (2022).
38. Liu, H. & Tang, T. Pan-cancer genetic analysis of Cuproptosis and copper metabolism-related gene set. *Front. Oncol.* **12**, 952290. <https://doi.org/10.3389/fonc.2022.952290> (2022).
39. Bao, J. H. et al. Identification of a novel cuproptosis-related gene signature and integrative analyses in patients with lower-grade gliomas. *Front. Immunol.* **13**, 933973. <https://doi.org/10.3389/fimmu.2022.933973> (2022).
40. Liu, Y., Luo, G., Yan, Y. & Peng, J. A pan-cancer analysis of copper homeostasis-related gene lipoyltransferase 1: its potential biological functions and prognosis values. *Front. Genet.* **13**, 1038174. <https://doi.org/10.3389/fgene.2022.1038174> (2022).
41. Ni, M. et al. Functional assessment of Lipoyltransferase-1 deficiency in Cells, Mice, and humans. *Cell. Rep.* **27**, 1376–1386e1376. <https://doi.org/10.1016/j.celrep.2019.04.005> (2019).
42. Cai, F. et al. Transcription factor GTF2B regulates AIP protein expression in growth hormone-secreting pituitary adenomas and influences tumor phenotypes. *Neuro Oncol.* **24**, 925–935. <https://doi.org/10.1093/neuonc/noab291> (2022).
43. Ruan, Z. et al. Overexpression of long non-coding RNA00355 enhances proliferation, chemotaxis, and metastasis in colon cancer via promoting GTF2B-mediated ITGA2. *Transl Oncol.* **14**, 100947. <https://doi.org/10.1016/j.tranon.2020.100947> (2021).
44. Kunadis, E., Lakiotaki, E., Korkolopoulou, P. & Piperi, C. Targeting post-translational histone modifying enzymes in glioblastoma. *Pharmacol. Ther.* **220**, 107721. <https://doi.org/10.1016/j.pharmthera.2020.107721> (2021).
45. Bryant, J. P., Heiss, J. & Banasavadi-Siddegowda, Y. K. Arginine Methylation in Brain Tumors: Tumor Biology and Therapeutic Strategies. *Cells* **10**, <https://doi.org/10.3390/cells10010124> (2021).
46. Song, L. & Luo, Z. Q. Post-translational regulation of ubiquitin signaling. *J. Cell. Biol.* **218**, 1776–1786. <https://doi.org/10.1083/jcb.201902074> (2019).
47. Guo, J. et al. Quantitative proteomics analysis reveals nuclear perturbation in human glioma U87 cells treated with Temozolomide. *Cell. Biochem. Funct.* **38**, 185–194. <https://doi.org/10.1002/cbf.3459> (2020).

Acknowledgements

We thank for all the participants for their participation and colleagues for their valuable assistance.

Author contributions

Jianping Zeng: Writing original draft, Validation, Project administration, Methodology, Investigation, Formal analysis, Data curation, Conceptualization. Jing Liu: Writing review& editing, Resources, Project administration, Conceptualization. Shushan Hua: Project administration, Supervision, Resources, Software. Shuai Liu: Writing review&editing, Supervision, Project administration. Shoufang Tong: Methodology, Investigation, Data curation. Jie Zhang: Rajneesh Mungur: Writing-review&editing. Shangshi Chen: Methodology, Investigation, Formal analysis, Jiugeng Feng: Supervision, Resources, Methodology, Investigation, Data curation. Cong Ding: Validation, Methodology, Investigation, Formal analysis, Data curation, Conceptualization.

Funding

This work was supported by the Natural Science Foundation of Jiangxi Province, China (No. 20242BAB25530); the Science and Technology Planning Project of Jiangxi Province, China (No. 202510252).

Declarations

Competing interests

The authors declare no competing interests.

Additional information

Supplementary Information The online version contains supplementary material available at <https://doi.org/10.1038/s41598-026-37105-w>.

Correspondence and requests for materials should be addressed to C.D.

Reprints and permissions information is available at www.nature.com/reprints.

Publisher's note Springer Nature remains neutral with regard to jurisdictional claims in published maps and institutional affiliations.

Open Access This article is licensed under a Creative Commons Attribution-NonCommercial-NoDerivatives 4.0 International License, which permits any non-commercial use, sharing, distribution and reproduction in any medium or format, as long as you give appropriate credit to the original author(s) and the source, provide a link to the Creative Commons licence, and indicate if you modified the licensed material. You do not have permission under this licence to share adapted material derived from this article or parts of it. The images or other third party material in this article are included in the article's Creative Commons licence, unless indicated otherwise in a credit line to the material. If material is not included in the article's Creative Commons licence and your intended use is not permitted by statutory regulation or exceeds the permitted use, you will need to obtain permission directly from the copyright holder. To view a copy of this licence, visit <http://creativecommons.org/licenses/by-nc-nd/4.0/>.

© The Author(s) 2026